



Assessing and enhancing Noah-MP land surface modeling over tropical environments

Yanyan Cheng^{1*}, Kalli Furtado¹, Cenlin He², Fei Chen³, Alan Ziegler⁴, Song Chen¹, Matteo Detto^{5,6}, Yuna Mao⁷, Baoxiang Pan⁸, Yoshiko Kosugi⁹, Marryanna Lion¹⁰, Shoji Noguchi¹¹, Satoru Takanashi¹²,
5 Lulie Melling¹³, Baoqing Zhang¹⁴

1 Centre for Climate Research Singapore, Singapore, Singapore

2 NSF National Center for Atmospheric Research, Boulder, Colorado, USA

3 Division of Environment and Sustainability, The Hong Kong University of Science and Technology, Hong Kong, Hong Kong, China

4 Faculty of Fisheries Technology and Aquatic Resources, Maejo University, Chiang Mai, Thailand

10 5 Department of Ecology and Evolutionary Biology, Princeton University, Princeton, New Jersey, USA

6 Smithsonian Tropical Research Institute, Panama City, Panama

7 State Key Laboratory of Earth Surface Processes and Resource Ecology, Faculty of Geographical Science, Beijing Normal University, Beijing, China

8 Institute of Atmospheric Physics, Chinese Academy of Sciences, Beijing, China

9 Laboratory of Forest Hydrology, Division of Forest and Biomaterials Science, Graduate School of Agriculture, Kyoto University, Kyoto, Japan

15 10 Forest Research Institute Malaysia, Kepong, Selangor, Malaysia

11 Tohoku Research Center, Forestry and Forest Products Research Institute, Iwate, Japan

12 Kansai Research Center, Forestry and Forest Products Research Institute, Kyoto, Japan

13 UN Sustainable Development Solutions Network, Asia Headquarters, Sunway University, Bandar Sunway, Selangor, Malaysia

14 Key Laboratory of West China's Environmental Systems (Ministry of Education), College of Earth and Environmental Sciences, Lanzhou University, Lanzhou, Gansu, China

20 *Correspondence to:* Yanyan Cheng (cheng_yanyan@nea.gov.sg)

Abstract. Despite the critical role of tropical land-surface processes in Earth system dynamics, large gaps persist in model evaluation and calibration for these regions. This study addresses this disparity through site-specific calibration of the Noah with Multi-Parameterizations (Noah-MP) land surface model at two tropical forest sites in Panama and Malaysia and one urban tropical site in Singapore. The site-specific calibration improves the model's ability to simulate key variables, including latent
25 and sensible heat fluxes as well as soil moisture, particularly at daily and seasonal scales. Sensitivity analyses identify consistently influential parameters across land cover types, offering guidance for model tuning in other tropical contexts. Nevertheless, challenges persist, particularly in estimating nighttime sensible heat fluxes, balancing the optimization of latent and sensible heat fluxes, and capturing seasonal soil moisture dynamics. These insufficiencies may be due to a lack of realistic complexity in Noah-MP's land-surface physics, including multi-species vegetation modeling, soil organic layer treatments,
30 subsurface hydrological processes, and permeable urban surfaces. Our results demonstrate how targeted parameter refinement can improve Noah-MP's performance in the tropics and inform future development priorities. These findings contribute to broader efforts to generalize model calibration strategies and improve Earth system model fidelity in data-scarce, climatically distinct regions.



1 Introduction

35 Land surface processes play a vital role in modulating regional and global climate dynamics through mechanisms such as evapotranspiration, the exchange of momentum, albedo, and greenhouse gas emissions (Bonan, 1995; Cheruy et al., 2014; Cox et al., 1999, 2000; Crossley et al., 2000; Dickinson, 1983; Lawrence et al., 2012; Lin et al., 2017; Mahmood et al., 2014; Pielke et al., 2011; Pitman et al., 2009; Unger, 2014; Van Weverberg et al., 2018). These processes are particularly critical in tropical regions, which act as key drivers of global climate systems (Gentine et al., 2019). Tropical forests, for instance, are the largest
40 terrestrial carbon sinks, regulating the Earth's climate by cycling vast amounts of carbon, water and energy (Pan et al., 2011; Schlesinger and Jasechko, 2014). Additionally, tropical land surfaces significantly impact local weather patterns, monsoon circulation, and extreme weather events such as tropical cyclones and intense convective storms (Gentine et al., 2019; Li et al., 2016). Understanding these processes is essential for predicting climate change and variability, managing water resources, and conserving biodiversity in these ecologically vital regions.

45 Recent rapid urbanization, deforestation, agricultural expansion, and wildfires across the tropical regions have profoundly altered land cover and land use patterns (Lambin et al., 2003; Vetruta and Cochrane, 2020). These changes have significant implications for surface energy, water, and carbon cycles, as they modify surface albedo, heat fluxes, soil moisture, vegetation covers, and local climate dynamics (Hasler et al., 2024; Sun et al., 2021). For instance, revegetation can enhance evapotranspiration, leading to a cooling effect (Shao and Zhang, 2019). However, reduced surface albedo associated with
50 revegetation may increase temperature by absorbing more shortwave radiation, potentially outweighing the cooling effect of increased evapotranspiration (Zhang et al., 2022). Such changes are particularly concerning in tropical regions, which are prone to extreme weather events like tropical cyclones, monsoon disturbances, and intense convective storms. Land surface processes can influence the development, intensity, and tracks of these events through feedback mechanisms involving surface moisture, heat fluxes, and atmospheric stability (Ma et al., 2013). Accurate representation of these changes in land surface and
55 land-atmosphere interactive processes is therefore crucial for improving early warning systems, disaster preparedness, and sustainable land management strategies.

Land surface models (LSMs) are essential tools for simulating and predicting these complex processes as well as their changes (Bonan and Doney, 2018). Over the years, LSMs have evolved from simplified representations of land surface biophysics to sophisticated frameworks that integrate biophysical, biogeochemical, hydrological, and ecological processes
60 (Fisher and Koven, 2020). They are widely used to assess the impacts of land-use changes on water and carbon cycles, evaluate land-atmosphere interactions, and inform strategies for managing the water-food-energy nexus (Cheng et al., 2022; Cheng et al., 2024a).

Despite recent advancements, LSMs are complex and still require extensive testing and calibration across diverse climate regimes. This issue relates to the fact that default parameterizations, which are often developed using mid-latitude
65 observational data, may not translate well to other biomes with fundamentally different environmental conditions (Lu et al., 2018, 2024). Each region (tropical, temperate, boreal, and arid) differs in key environmental and biological processes, and land



cover types such as forests, grasslands, and urban areas exhibit distinct land-atmosphere interactions. Consequently, using default configurations could lead to poor representation of temporal variability in surface fluxes (e.g., latent and sensible heat, photosynthesis) and misrepresentation of biogeochemical and hydrological processes (e.g., soil moisture and streamflow dynamics) (Lu et al., 2018, 2024).

This challenge is pronounced in tropical regions, where high biodiversity, complex canopy structures, and distinct wet-dry seasonality complicate model performance. For example, representing tropical forest diversity in land surface models remains challenging due to limited understanding of the mechanisms underlying forest functional diversity. In particular, few studies have calibrated the ecological coexistence of tropical tree species, which are the processes that allow multiple species with differing traits to persist together over time within the same ecosystem (Yanyan Cheng, Wang, et al., 2024b). Moreover, the critical role of soil hydrological processes in shaping tropical ecosystem behavior has been underexplored in model calibration efforts (Cheng et al., 2022; Cheng et al., 2023; Cheng et al., 2024b).

To address these limitations, site- or region-specific calibration is essential for improving model accuracy and ensuring reliable simulations at local, regional, and global scales (Cheng et al., 2023; Huang et al., 2016; Lu and Ricciuto, 2019; Müller et al., 2015; R. Sun et al., 2021). Particularly important is the joint tuning of soil and vegetation parameters and validation across multiple timescales, especially in regions with pronounced seasonal variability such as the tropics (Ogden et al., 2013). Without such targeted calibration, LSMs are likely to struggle to accurately simulate key variables like surface energy fluxes, vegetation dynamics, and land-atmosphere interactions.

The objective of this study is to assess and enhance the performance of the widely-used Noah with Multi-Parameterization options (Noah-MP) LSM in tropical regions. Noah-MP stands out for its versatility and comprehensive treatment of land surface processes (Chang et al., 2020; He et al., 2023a; Niu et al., 2011; Yang et al., 2011). Its multi-physics framework facilitates the incorporation of diverse parameterizations, enabling its applications across a wide range of environmental conditions. Its seamless integration with numerical weather prediction (NWP) models, such as the Weather Research and Forecasting (WRF) model, the Multiscale Prediction and Analysis System (MPAS), and NOAA's Unified Forecast System (UFS), significantly enhances its utility in climate and weather simulations. However, despite its widespread use, Noah-MP applications remain understudied in tropical environments. In this study, we evaluate and calibrate Noah-MP against observational data from three tropical field sites: two forest sites in Panama and Malaysia, and one urban site in Singapore. We assess the model's ability to simulate diurnal, daily, and seasonal dynamics of land surface energy fluxes and soil moisture. Recognizing that Noah-MP's performance is sensitive to the choice of key vegetation and soil parameters, we explicitly calibrate them to improve representation of tropical ecosystem dynamics.



2 Methods and data

2.1 Study area and field data for model evaluation and calibration

We use observational data from three tropical sites, including two tropical forest sites (Panama and Malaysia) and a tropical urban site (Singapore) (Figure 1, Table 1), to calibrate Noah-MP and improve its performance over tropical regions. Specifically, we evaluate and improve Noah-MP's performance in simulating latent heat (LH), sensible heat (SH), and soil moisture (SM), which are key variables influencing land-atmosphere interactions.

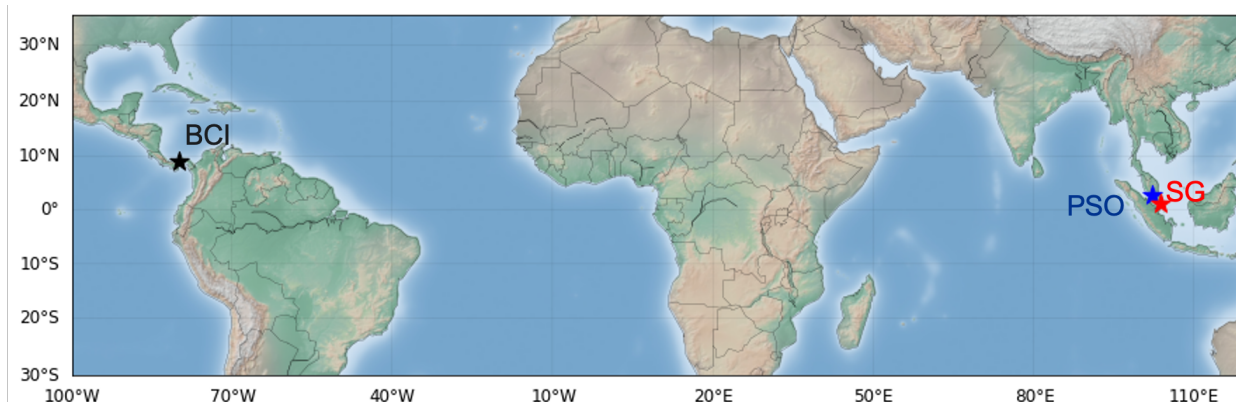


Figure 1. Locations of the study sites include a tropical forest site in Barro Colorado Island, Panama (BCI, black star), a tropical forest site in Pasoh Forest Reserve, Malaysia (PSO, blue star), and a tropical urban site in Singapore (SG, red star).

Table 1. Detailed information for the three study sites.

	Panama BCI	Malaysia PSO	Singapore
Latitude	9.151	2.9667	1.3143
Longitude	-79.855	102.3	103.9112
Vegetation	Evergreen broadleaf forest	Evergreen broadleaf forest	Forest and urban
Data availability	20150730 ~ 20170831	20030101 ~ 20091231	20060430 ~ 20070331
Wind speed (m/s)	2.94	1.86	2.09
Temperature (°C)	25.5	25.3	27.4
Humidity	89.0 %	82.9 %	0.016 kg/kg
Air pressure (mb)	988	989	1008
Shortwave radiation (W/m ²)	195	198	371
Longwave radiation (W/m ²)	428	419	415
Precipitation (mm/year)	2025	1790	2524
Latent heat (W/m ²)	70.5	99.2	36.5



Sensible heat (W/m^2)	30.3	44.7	55.1
----------------------------------	------	------	------

2.1.1 Panama tropical forest site

The Barro Colorado Island (BCI) site in Panama is located at 9.151°N , 79.855°W . It is a primary lowland (elevation 120 m) semi-deciduous tropical forest site with a mean canopy height of 30 and few emergent trees (Cheng et al., 2022; Detto et al., 2015; Detto and Pacala, 2022; Fang et al., 2022). It has distinct dry (mid-December to mid-April) and wet (late-April to early December) seasons (Ogden et al., 2013). The site exhibits a tropical monsoon climate (Am), characterized by a short dry season. The soils are mostly well weathered kaolinitic Oxisols. Meteorological and flux data were collected from a 45 m tower located on the top-plateau at a half-hour temporal resolution (Detto and Pacala, 2022). The mean annual precipitation, wind speed, air temperature, relative humidity, air pressure, shortwave radiation, and longwave radiation during 2015 to 2017 are 2025 mm, 2.94 m/s, 25.5°C , 89%, 98.8 kPa, 195 W/m^2 , and 428 W/m^2 , respectively (Table 1). The soil moisture is measured in the top 15 cm of the soil (Cheng et al., 2022; Detto and Pacala, 2022).

2.1.2 Malaysia tropical forest site

The Pasoh Forest Reserve (PFR), known as the PSO AsiaFlux site, is a tropical forest located in Malaysia at 2.9667°N , 102.3°E . This lowland forest (140 m elevation) boasts a canopy height of 30 ~ 40 m, with emergent trees reaching 45 m. The site is notable for being located within a dry zone of Peninsular Malaysia and receives the lowest annual rainfall among adjacent south-eastern tropical rainforests (Lion et al., 2017; Noguchi et al., 2016). The soils are dominated by Ultisols and Oxisols, which are Haplic Acrisol and Xanthic Ferralsol in FAO classification. The site has a tropical rainforest climate (Af), with consistently high rainfall throughout the year.

The observed data were measured at a height of 54 m on the flux tower at a half-hour temporal resolution (Lion et al., 2017). The mean annual precipitation, wind speed, air temperature, relative humidity, air pressure, shortwave radiation, and longwave radiation from 2003 to 2009 are 1790 mm, 1.86 m/s, 25.3°C , 82.9%, 98.9 kPa, 198 W/m^2 , 419 W/m^2 , respectively (Table 1). The volumetric soil water content is calculated as the average of observations from nine time domain reflectometry (TDR) sensors placed at depths of 10, 20, and 30 cm at three locations around the flux tower (Noguchi et al., 2016).

2.1.3 Singapore tropical urban site

The Singapore (SG) tropical urban site is located at 1.3143°N , 103.9112°E . It is a compact low rise residential site (Lipson et al., 2022; Roth et al., 2017). The eddy covariance flux tower is located on the grounds of a student hostel, in the southwest corner of a grass-covered sports field. Within a 1000 m radius of the eddy covariance tower, the surface consists of a mix of impervious areas, including buildings, roads, and parking lots, and pervious areas, including trees and grass (Roth et al., 2017). The flux tower observational data have a half-hour temporal resolution. The mean annual precipitation, wind speed, air



temperature, specific humidity, air pressure, shortwave radiation, and longwave radiation from 2006 to 2007 are 2524 mm, 2.09 m/s, 27.4 °C, 0.016 kg/kg, 100.8 kPa, 371 W/m², and 415 W/m², respectively (Table 1).

2.2 Noah-MP

The community Noah-MP LSM (He et al., 2023a, 2023b; Niu et al., 2011) is designed for a wide range of applications, including uncoupled studies of hydrometeorological and ecohydrological processes, as well as coupled numerical weather prediction and decadal climate simulations. It can operate from point to global scales. The land grid in Noah-MP is divided into two sub-grid tiles: vegetated and non-vegetated areas, determined by vegetation cover fraction. The biogeophysical and biogeochemical processes are treated separately for these two tiles. Noah-MP employs a “big-leaf” canopy approach, with canopy properties varying according to the type of vegetation (He et al., 2023a).

For urban applications, the single-layer urban canopy model (SLUCM) in the integrated Weather Research and Forecasting (WRF)-urban modeling system (F. Chen et al., 2011) has been coupled with Noah-MP (Salamanca et al., 2018), allowing the offline (standalone) Noah-MP-SLUCM simulation.

More detailed descriptions of Noah-MP and SLUCM have been provided elsewhere (Chen et al., 2011; He et al., 2023c). The Noah-MP-SLUCM model has been applied to various urban environments by previous studies (Gao et al., 2019; Newman et al., 2024; Xue et al., 2024).

2.3 Model simulations

We configure single-point Noah-MP simulations at the three study sites and calibrate the model at the daily scale. For the Panama tropical forest site, the vegetation type is set as evergreen broadleaf forest and the soil type as clay. The simulated soil moisture for the top 10 cm is used as the closest available depth for validation against the observations at the site in Panama. At the Malaysia site, the vegetation type is also evergreen broadleaf forest, with silty clay soil. The simulated soil moisture averaged over the top 30 cm is used to validate against the observed soil water content at the site. For the Singapore tropical urban site, the vegetation is defined as a mix of urban and grassland, with their fractions determined by the model’s urban fraction parameter.

2.4 Sensitivity analysis

We select several key vegetation and soil parameters for sensitivity analysis and calibration based on the past experience and literature reports (Arsenault et al., 2018) (Table 2), which include the maximum rate of carboxylation at 25 degC (VCMX25), leaf area index (LAI), top of canopy (HVT), bottom of canopy (HVB), momentum roughness length (Z0MVT), empirical canopy wind absorption parameter (CWPVT), saturated value of soil moisture (MAXSMC), saturated hydraulic conductivity (SATDK), wilting point (WLTSMC), and field capacity (REFSMC). For vegetation parameters, VCMX25 regulates the photosynthesis rate and stomatal resistance, LAI is related to plant phenology, and HVT and HVB determine canopy thickness. CWPVT affects turbulent heat transfer below canopies, while Z0MVT controls sensible and latent heat fluxes above the



canopy. For soil parameters, MAXSMC, WLTSMC, and REFSMC determine soil water retention and the amount of water available for plant uptake, while SATDK controls the infiltration rate.

170 **Table 2.** Noah-MP parameters used in the sensitivity analysis.

Parameter	Full name	Relevant process	Bound	Reference
VCMX25	Maximum rate of carboxylation at 25 degC (umol CO ₂ /m ² /s)	Photosynthesis rate	30 ~ 120	Domingues et al., (2005); Chen et al., (2008)
HVT	Top of canopy (m)	Plant transpiration	9 ~ 55	Kosugi et al., (2012)
HVB	Bottom of canopy (m)	Plant transpiration	0.1 ~ 15	Kosugi et al., (2012)
CWPVT	Empirical canopy wind absorption parameter	In and below canopies sensible heat	0.15 ~ 5.35	Goudriaan (1977)
Z0MVT	Momentum roughness length (m)	Above-canopy sensible heat	0.0 ~ 1.1	He et al., (2023)
LAI	Leaf area index (m ² /m ²)	Phenology	1 ~ 8	Kosugi et al., (2012)
WLTSMC	Wilting point (m ³ /m ³)	Soil moisture	0.02 ~ 0.26	Marryanna et al., (2019)
REFSMC	Field capacity (m ³ /m ³)	Soil moisture	0.15 ~ 0.45	Litt et al., 2020 (2020)
MAXSMC	Saturated value of soil moisture (m ³ /m ³)	Soil moisture	0.45 ~ 0.75	Litt et al., 2020 (2020)
SATDK	Saturated hydraulic conductivity (m/s)	Soil moisture	$8.9 \times 10^{-6} \sim 5 \times 10^{-4}$	Marryanna et al., (2019)

We examine the sensitivity of Noah-MP-simulated land surface conditions to these key parameters by conducting a linear univariate sampling of their values within predefined uncertainty ranges (Table 2) (Cheng et al., 2020; Kennedy et al., 2024). Specifically, each parameter is varied incrementally (10 values with equal intervals) while keeping the remaining parameters fixed at their default values as given in Tables 3-4.

To select optimal parameter values, we adopt field-reported values for parameters with available measurements (e.g., LAI). For the other parameters, we use the results from the sensitivity analysis to select the optimal parameter values that yield the lowest bias between daily site-level measurements and model simulations. These calibrated parameter values are used for subsequent analyses and discussions.

180 We rank the importance of the parameters for energy fluxes using the following equation, which evaluates the individual contribution of a single parameter when varied, relative to the total variation observed using the default parameter set.



$$S_j^i = \left| \frac{V_j^{linear_sampling,i} - V_{observed,j}}{V_{default,j} - V_{observed,j}} \right| \quad (1)$$

where $V_j^{linear_sampling,i}$ is the Noah-MP output j (LH or SH) when only parameter i is perturbed (while others remain at default values), $V_{default,j}$ is the model output j using all default parameter values, $V_{observed,j}$ is the observed value for variable j (i.e., LH or SH). The metric S_j^i represents the sensitivity of variable j to parameter i . Parameters are ranked by the magnitude of S_j^i , with higher values indicating greater impact on the model output.

3 Results

For each site, our analysis includes a discussion of parameter sensitivity results to identify the most influential parameters and their optimal values. We also examine how calibrating these parameters affects day-to-day variability, as well as seasonal and diurnal cycles.

3.1 Tropical forests sites

3.1.1 Panama tropical forest site

At the Panama BCI tropical forest site, we find that the most important parameter for LH and SH is the maximum rate of carboxylation at 25 degC (VCMX25) (Table 3), which controls the photosynthesis rate and stomatal conductance, and thereby also plays a dominant role in both carbon assimilation and evapotranspiration. The calibrated VCMX25 value is 100 $\mu\text{mol}/\text{CO}_2/\text{m}^2/\text{s}$. This is consistent with other studies that have identified the typical values of VCMX25 for Panama BCI tropical forests (Cheng et al., 2024b). While VCMX25 modulates both heat fluxes by altering LH, with subsequent change in SH via energy partitioning, Z0MVT is also important for directly controlling above-canopy sensible heat, which induces a latent heat response by cooling the land surface. SATDK plays a key role in regulating latent heat, as it determines the amount of water available for plants to uptake.

Table 3. Default and calibrated parameter values at the Panama BCI tropical forest site.

Parameter	Default value	Calibrated value	Rank of importance for LH	Rank of importance for SH
VCMX25	60	100	1	1
HVT	20	45	5	3
HVB	8	25	5	3
Z0MVT	1.1	0.8	2	2
MAXSMC	0.468	0.525	4	4



SATDK	9.74×10^{-5}	1×10^{-4}	3	5
-------	-----------------------	--------------------	---	---

The calibrated parameters improve the simulation of daily soil moisture and SH at the Panama tropical forest site (Figure 2). For soil moisture, the observed mean value is $0.398 \text{ m}^3/\text{m}^3$. Simulations using default and calibrated parameters yield mean soil moisture values of $0.367 \text{ m}^3/\text{m}^3$ and $0.395 \text{ m}^3/\text{m}^3$, respectively. The mean bias for soil moisture decreases from $-0.031 \text{ m}^3/\text{m}^3$ for default parameterization to $-0.003 \text{ m}^3/\text{m}^3$ for calibrated parameterization. The coefficient of determination (R^2) values for soil moisture increase from 0.49 for the default parameterization to 0.73 for the calibrated parameterization (Figure S1).

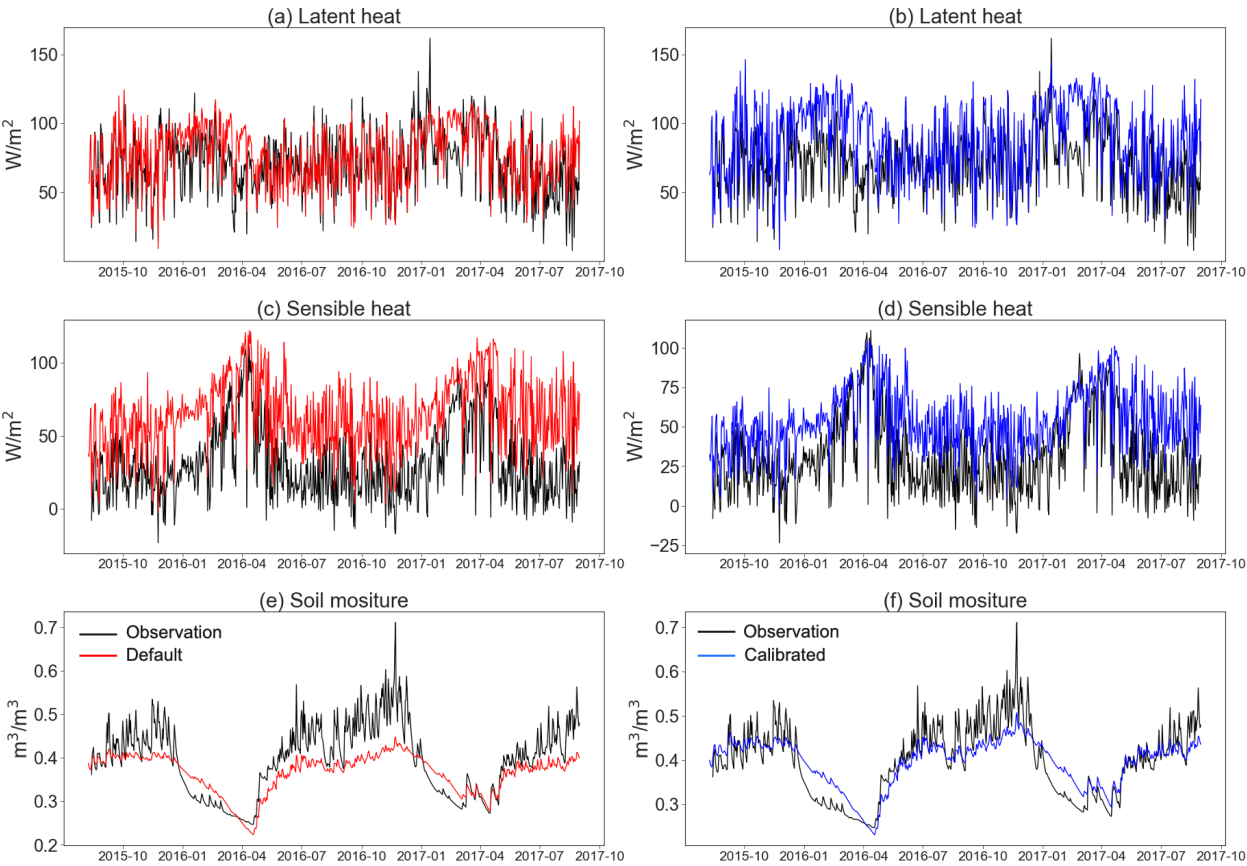


Figure 2. Observation (black line) and daily simulation results at the Panama BCI tropical forest site for (a-b) latent heat, (c-d) sensible heat, and (e-f) soil moisture, using default parameters (left column, red line) and calibrated parameters (right column, blue line).

For LH and SH, the observed mean values are 70.5 W/m^2 and 30.3 W/m^2 , respectively (Table 1). The simulation using default parameter values yields mean LH and SH values of 76.5 W/m^2 and 64.7 W/m^2 , respectively, while the simulation using calibrated parameter values produces mean LH and SH values of 87.6 W/m^2 and 53.8 W/m^2 , respectively. The mean biases



for LH and SH are 6.0 W/m^2 and 34.4 W/m^2 for the default parameterization, compared to 17.1 W/m^2 and 23.5 W/m^2 for the calibrated parameterization.

Noah-MP effectively captures the seasonal and diurnal dynamics of surface energy and water fluxes for both model configurations (Figure 3). Specifically, it captures the decline in LH and soil moisture, as well as the corresponding peak in SH around April (Figures 3a and 3c). However, the model does not fully capture the peak in soil moisture from September to November (Figure 3e), consistent with its deficiencies in simulating wet-season soil moisture peaks as observed in the daily results (Figure 2f). The underestimated wet-season soil moisture may be caused by the deficiencies in subsurface water transport representation, such as the absence of preferential flow simulation in Noah-MP, which is known to govern seasonal sub-surface fluxes of water in tropical rainforests by rapidly transporting water downward (Cheng et al., 2017, 2018, 2019). Preferential flow paths generated by tree root penetration, termite activity, earthworm burrows, or other soil microporosity significantly alter the partitioning of water and energy, affecting not only runoff, but also water storage and plant water uptake, which reflects in the surface-air water fluxes. Therefore, their absence in Noah-MP could be an important source of structural error which would further hinder calibrations based on heat fluxes. This critical process has received insufficient attention in the context of land surface modeling and deserves future model development efforts.

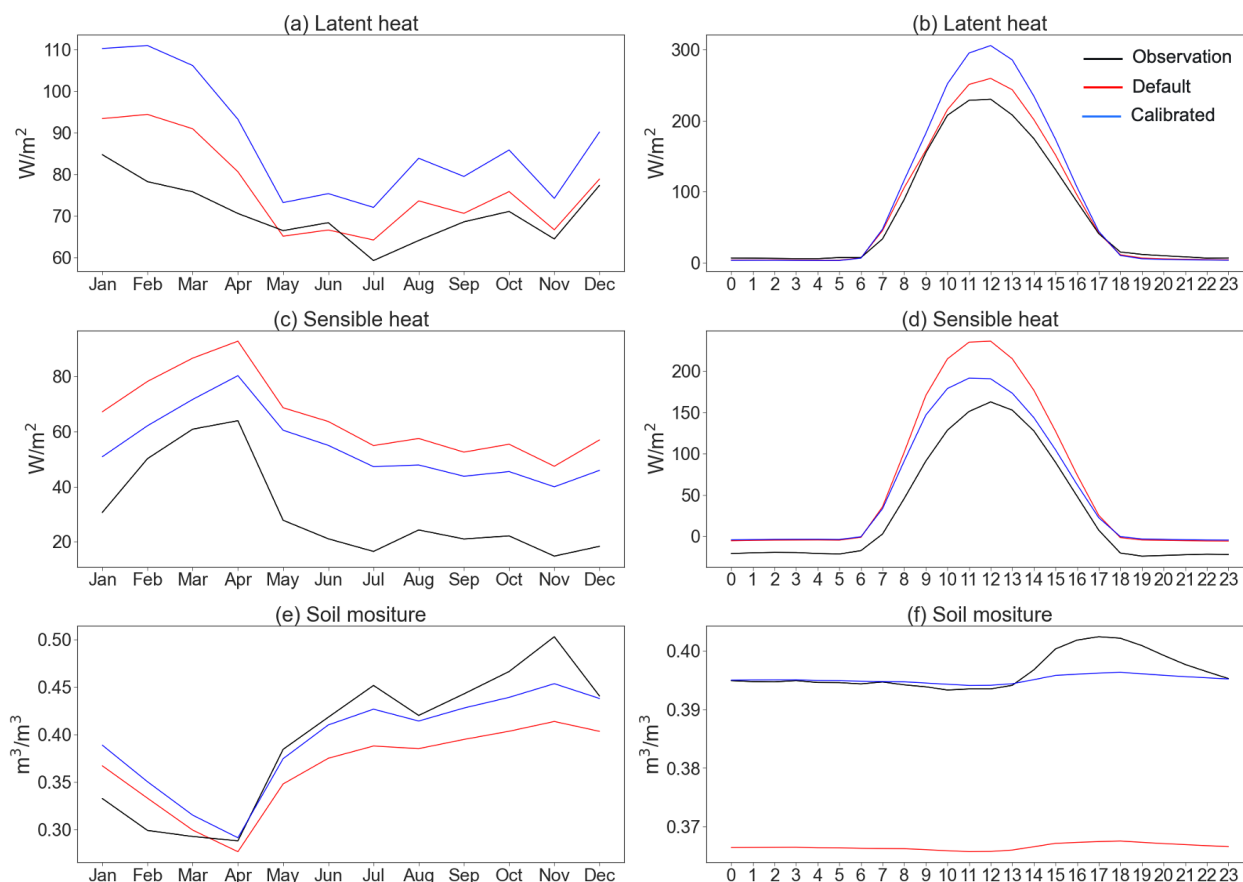




Figure 3. Observation (black line) and simulation results at the Panama BCI tropical forest site for (a-b) latent heat, (c-d) sensible heat, and (e-f) soil moisture, using default parameters (red line) and calibrated parameters (blue line) for seasonal (left column) and diurnal (right column) cycles.

235

There is a trade-off in optimizing LH and SH, at seasonal, daily, and diurnal scales (Figures 2-3), making it challenging to simultaneously capture the dynamics of both fluxes. Compared to the results using default parameters (Figures 2a and 2c, Figures 3a-d), the calibrated parameters improve the simulation performance for SH (Figures 2d and 3d) but undermine the performance for LH (Figures 2b and 3b). This is further evident when examining the correlations between predicted and observed LH and SH (R^2) as we reported earlier (Figure S1). For example, with default parameters there is a better linear correlation between simulated and observed daily means of LH ($R^2 = 0.51$). For the calibrated parameters, a positive correlation is retained, but a positive LH bias develops on days when the LH flux is relatively large (Figure S1b). This can also be seen in the daily time series and seasonal cycles (Figures 2-3) which show that LH overestimation is most severe between January and April, as the dry season develops but simulated LH remains relatively large. We note from Figures 2e-f that the dry down of soil moisture at these times of year is poorly captured, with both the calibrated and uncalibrated models overestimating soil moisture by an average of $0.03 \text{ m}^3/\text{m}^3$, which may explain why the calibration is ineffective at addressing LH biases. Additionally, downward solar radiation measured by the flux tower may contain biases. If it is overestimated, this could contribute to the overall overestimation of both latent and sensible heat fluxes.

Another possible source of the discrepancy between calibrated LH and SH may be Noah-MP's inability to simulate forest functional diversity, which are prevalent in tropical forests and critical for capturing forest response to environmental variability (Cheng et al., 2024b). Addressing this limitation may require the use of more advanced ecosystem demography models to better capture the interactions of multi-species coexistence in tropical ecosystems.

The model persistently overestimates nighttime SH (Figure 3d), which is consistent with an overestimation of nighttime soil temperature relative to observations (Figure S2). This discrepancy likely stems from the absence of a parameterization for the soil organic layer in Noah-MP. Organic layers, with their low thermal conductivity and high heat capacity, dampen both daytime heating and nocturnal cooling. Without this buffering effect, the model likely exaggerates diurnal soil temperature amplitudes, inflating both daytime peaks and nighttime minima. This structural limitation, which has been recognized in previous evaluations (Zhang et al., 2021), contributes to systematic SH biases and highlights a priority area for future model development.

260 3.1.2 Malaysia tropical forest site

The single most sensitive parameter for calibrating LH and SH at the Malaysia PSO tropical forest site is LAI (Table 4), but this parameter is considered to be relatively known, based on the site measurements (Kosugi et al., 2012). Therefore, as described in the Methods, the LAI value was updated from the Noah-MP default value for evergreen broadleaf forest ($4.5 \text{ m}^2/\text{m}^2$) to a field value of $6.52 \text{ m}^2/\text{m}^2$ (Table 4). The empirical canopy wind absorption parameter (CWPVT) is also important



265 for calibrating both LH and SH as it controls turbulent heat fluxes below the forest canopy. A set of soil parameters, including REFSMC, WLTS MC, and SATDK, strongly influence Noah-MP's simulation of energy and water fluxes by shaping how plant-available soil moisture is represented in the model.

Table 4. Default and calibrated parameter values at the Malaysia PSO tropical forest site.

Parameter	Default value	Calibrated value	Rank of importance for LH	Rank of importance for SH
VCMX25	60	58	6	6
HVT	20	45	7	7
HVB	8	20	7	7
CWPVT	0.67	0.3	2	5
LAI	4.5	6.52	1	1
WLTS MC	0.126	0.2186	8	4
REFSMC	0.404	0.3458	3	2
MAXSMC	0.468	0.4688	5	8
SATDK	1.34×10^{-4}	4×10^{-4}	4	3

270

The calibrated parameters substantially improve the simulation of energy and water fluxes at the Malaysia PSO tropical forest site (Figure 4). Specifically, at the daily scale, the observed mean LH and SH fluxes from 2003 to 2009 are 99.2 W/m² and 44.7 W/m², respectively (Table 1). The Noah-MP simulation using default parameter values yields mean LH and SH values of 85.0 W/m² and 53.5 W/m², while the simulation using calibrated parameter values produces mean LH and SH values of 96.9 W/m² and 43.6 W/m². The mean biases for LH and SH are -14.2 W/m² and 8.8 W/m² for default parameterization, compared to -2.3 W/m² and -1.1 W/m² for calibrated parameterization. Calibration also substantially improves the correlation between simulated and observed daily mean values of both LH and SH (Figure S3), with R² values for LH and SH increasing from 0.24 (LH) and 0.55 (SH) using default parameters, to 0.63 for both LH and SH after calibration (Figure S3).

275

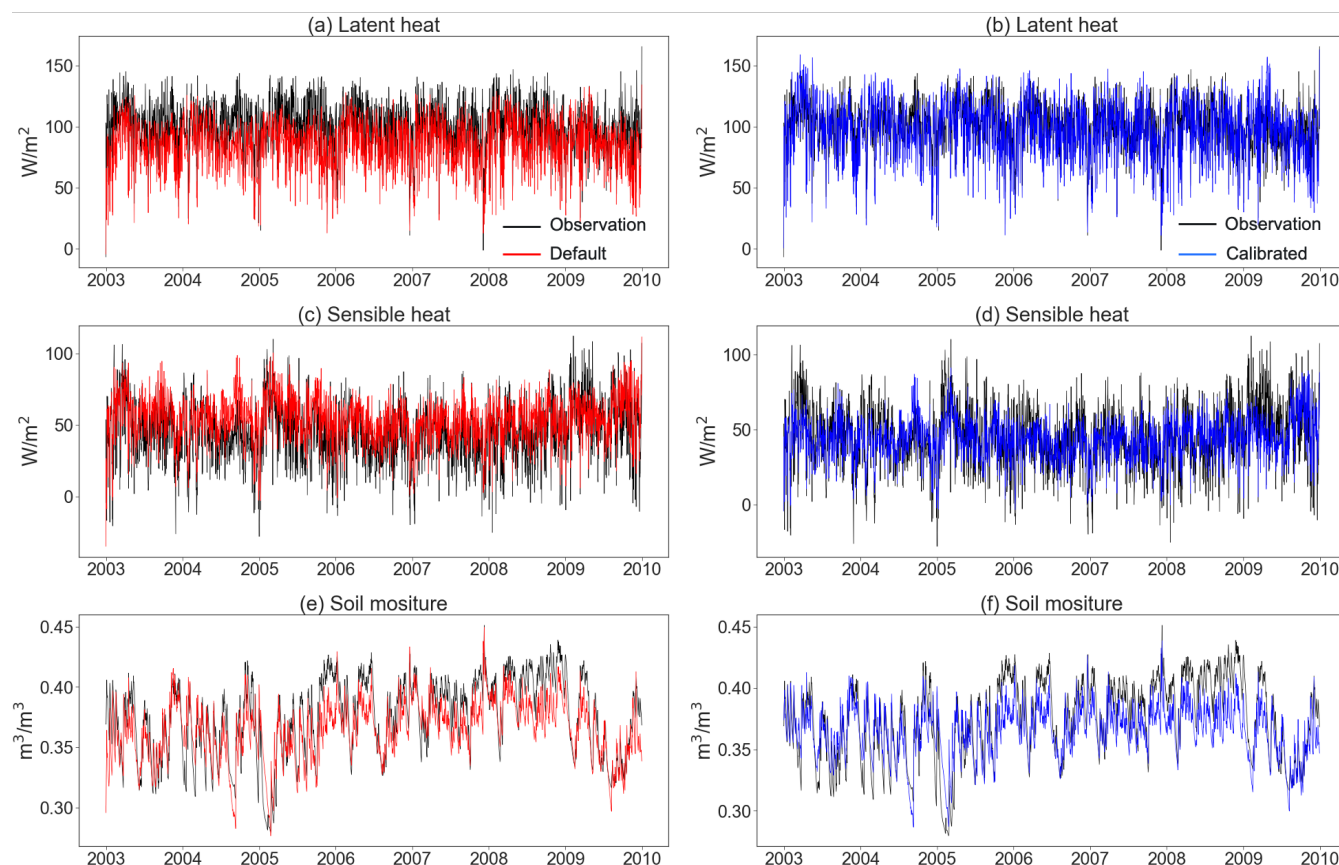


Figure 4. Observation (black line) and daily simulation results at the Malaysia PSO tropical forest site for (a-b) latent heat, (c-d) sensible heat, and (e-f) soil moisture, using default parameters (left column, red line) and calibrated parameters (right column, blue line).

For soil moisture, the observed mean value is $0.375 \text{ m}^3/\text{m}^3$. Soil moisture variability is reasonably well simulated by both configurations with mean biases of $-0.011 \text{ m}^3/\text{m}^3$ for default parameterization and $-0.01 \text{ m}^3/\text{m}^3$ for calibrated parameterization (Figures 4e-f). The R^2 values for soil moisture are similar for default (0.64) and calibrated results (0.6) (Figure S3). Compared to fluxes, the improvement in soil moisture simulation is less pronounced, likely due to the relatively small differences between the calibrated and default values of parameters governing soil moisture dynamics (e.g., MAXSMC) (Table 4). Overall, calibration attempts can be considered more successful for PSO in Malaysia than for BCI in Panama, possibly because the weaker seasonality at the Malaysia site means that the models do not need to capture distinct wet-dry transitions.

In addition to daily dynamics, Noah-MP also adequately captures both seasonal and diurnal dynamics of energy and water fluxes at the PSO site (Figure 5). At the seasonal scale, both model configurations capture the decline in LH from April to July and from September to December (Figures 5a and 5c). Calibration greatly improves the simulation of LH, by removing a substantial underestimate that is present for all months with the default parameters. SH is similarly improved, except between February and April, when the decrease in SH due to calibration leads to an underestimation.

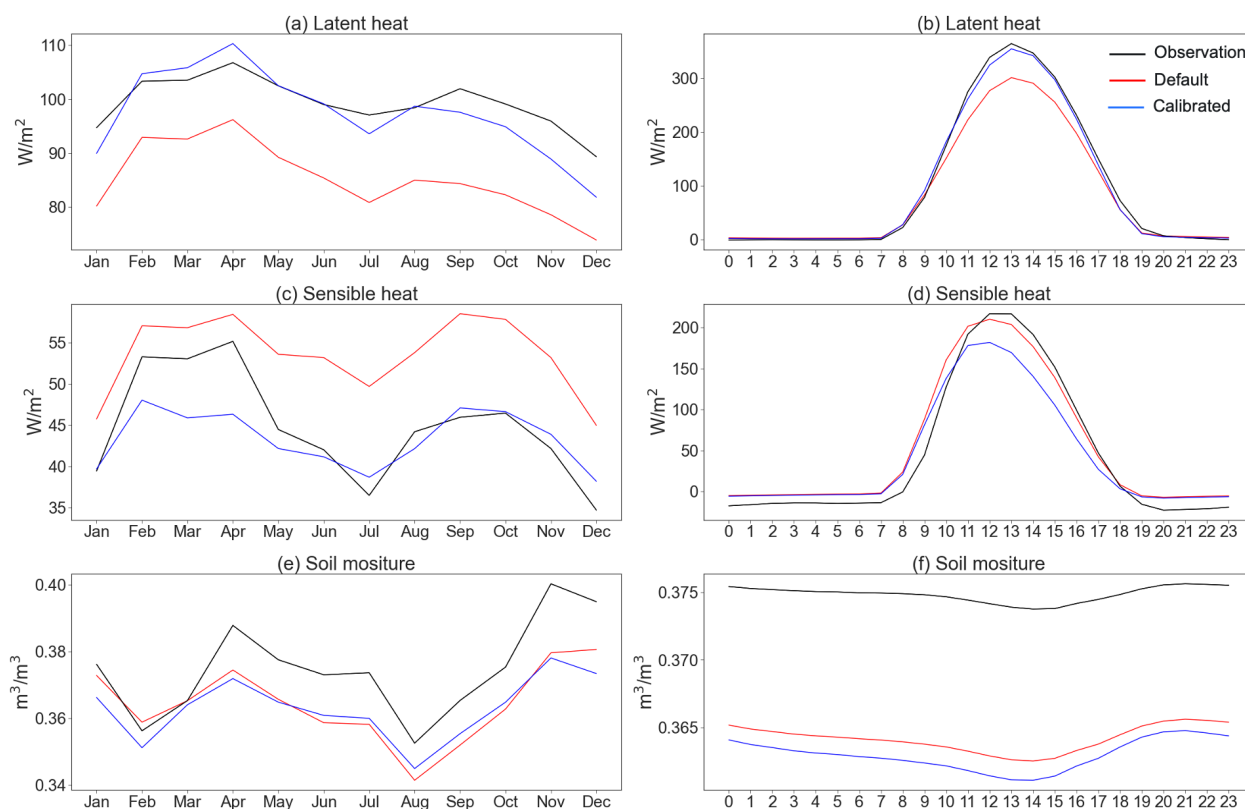


Figure 5. Observation (black line) and simulation results at the PSO tropical forest site for (a-b) latent heat, (c-d) sensible heat, and (e-f) soil moisture, using default parameters (red line) and calibrated parameters (blue line) for seasonal (left column) and diurnal (right column) cycles.

At the diurnal scale, Noah-MP captures the peaks in LH (Figure 5b) and SH (Figure 5d) around noon time for both model configurations. For LH, calibration improves the simulations, indicating that calibration on daily timescales translates into sub-daily improvements. Interestingly, for SH, the peak of the diurnal cycle is underestimated after calibration, even though the overall performance on daily and seasonal timescales is improved. This stems from the period from February to April, when the calibrated SH values are further reduced relative to the default, resulting in greater underestimation compared to observations. The variation in model performance in capturing the diurnal cycle across seasons clearly reveals this contrast. Specifically, from February to April, calibration increases the SH mean bias from $-3.6 W/m^2$ (default) to $+7.1 W/m^2$. While in the remaining months, calibration reduces the mean bias from $-10.5 W/m^2$ (default) to $-0.4 W/m^2$.

The notable success of co-calibration of both heat fluxes at PSO in Malaysia, compared to the conflicting results for LH and SH at BCI in Panama, is perhaps due to the large differences in climate and vegetation conditions between the two locations. Specifically, Panama has a tropical monsoon climate (Am), characterized by distinct dry and wet seasons, while Malaysia experiences a tropical rainforest climate (Af), with consistently high rainfall throughout the year. Furthermore, despite receiving less rainfall, the PSO site exhibits higher LH than the BCI site (Table 1), suggesting that structural vegetation



differences, such as LAI and canopy wind effects (represented at PSO by the sensitivity of the model to CWPVT), are playing a significant role in energy fluxes. For example, the positive LH biases at PSO with default parameters may be partially a result of underestimated damping of in-canopy winds by the relatively denser canopy, in which case calibrating CWPVT and LAI can be expected to improve both LH and SH. As a result, the parameters for the BCI site are not applicable to the PSO site. This highlights the importance of local observational data to guide the calibration. Nevertheless, the calibrated parameter values and their sensitivities can still offer useful insights for other tropical forest sites with similar climate regimes.

3.2 Singapore tropical urban site

The Singapore site is one of the few urban sites located in tropical regions (Lipson et al., 2022). The reported urban fraction for this region is 85% (Lipson et al., 2022; Roth et al., 2017); however, using this value leads to a substantial underestimation of LH in Noah-MP-SLUCM simulations (Figure 6a). To improve model performance, we adjusted the urban fraction to 70%—a value more consistent with high-resolution land cover data—and found that this change significantly improved the accuracy of LH simulations. Specifically, the observed mean LH value is 36.5 W/m^2 (Table 1). Noah-MP-SLUCM simulations with default parameters yield a mean LH of 14.2 W/m^2 , whereas the calibrated setup with a 70% urban fraction increases the mean LH to 27.2 W/m^2 . This reduces the LH mean bias from -22.3 W/m^2 (default) to -9.3 W/m^2 . The coefficient of determination (R^2) for LH improves from a negative value (-2.0 , indicating the model performs worse than simply using the mean of the observation for prediction) under default parameters to 0.14 with calibration (Figure S4), indicating a modest, though still limited, improvement in explained variance.

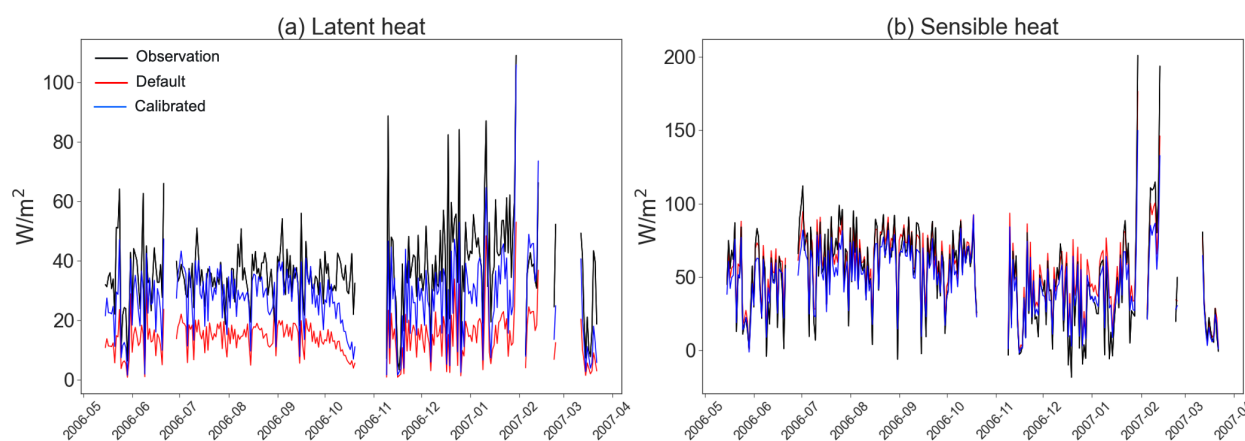


Figure 6. Observation (black line) and daily simulation results at the SG tropical urban site for (a) latent heat and (b) sensible heat, using default parameters (red line) and calibrated parameters (blue line). The gaps are due to missing data.

To validate the adjusted urban fraction, we analyzed the 100 m land use classification data for Singapore across buffer zones ranging from 100 m to 900 m around the flux site. The estimated urban fractions across these scales range from 46% to 77%, supporting the appropriateness of the 70% value used in our calibrated configuration.



One contributing factor is the simplified treatment of urban hydrology in SLUCM. In SLUCM, all rainfall on urban surfaces is entirely converted to surface runoff, no water is retained for infiltration, soil water storage, or evapotranspiration, making latent heat flux almost entirely dependent on the assumed urban fraction and surface roughness. This framework may be particularly inadequate in tropical cities like Singapore, where vegetation-lined streets, porous green infrastructure, and irrigated urban vegetation all influence evapotranspiration and surface fluxes. Moreover, the complex 3D geometry of tropical urban canopies, coupled with persistent high humidity and radiation loads, may induce heat flux behavior that current models do not fully resolve.

In contrast to LH, SH is relatively less sensitive to the urban fraction adjustment, as evidenced by similar evaluation metrics for both default and calibrated parameters. The observed mean SH is 51.1 W/m^2 . Simulations with default and calibrated parameters yield mean SH values of 55.0 W/m^2 and 47.5 W/m^2 , respectively. The corresponding biases are 3.9 W/m^2 and -3.6 W/m^2 , while R^2 values remain high at 0.88 and 0.85 for default and calibrated parameterizations, respectively (Figure S4), indicating that SH is generally well captured under both configurations. This lower sensitivity arises because SH differs less between urban and non-urban surfaces in Noah-MP, whereas LH is nearly zero over urban areas (Figure 6a); thus, even small changes in urban fraction can significantly alter grid-mean LH but have a minimal impact on grid-mean SH.

Compared to the forest sites, where biophysical processes such as soil moisture retention, root water uptake, and canopy turbulence can be tuned through multiple calibrated parameters, the SLUCM-based urban representation is more rigid. Consequently, improvements at the Singapore site are limited not by parameter uncertainty, but by structural model assumptions. Future efforts may benefit from coupling Noah-MP-SLUCM with explicit urban hydrology modules or replacing it with more flexible urban canopy schemes that include subsurface water routing and anthropogenic water inputs, such as the multilayer Building Effect Parameterization (BEP) and the Building Energy Model (BEM) (Salamanca et al., 2018). Future studies could assess the performance of these advanced urban schemes in tropical urban environments and investigate their impact on simulating urban heat islands and heatwave cases.

4. Additional Discussions

4.1 Future directions

This study serves as a foundational step toward enhancing Noah-MP's performance in tropical regions by calibrating the model using data from three distinct sites: a tropical forest site in Malaysia, a tropical forest site in Panama, and a tropical urban site in Singapore. Building on these findings, future research could focus on the following key areas to further advance Noah-MP's capabilities and applications over the tropics.

4.1.1 Regional calibration and application

Future work could extend calibration efforts to a broader regional scale across the tropical areas such as such as peat-swamp forests and Mangroves, which have distinct carbon cycles. Such efforts would significantly improve the accuracy of regional



weather forecasts and the reliability of regional climate projections for this region, but would need to rely heavily on remote sensing, given the scarcity of in situ measurements. Regional calibration would also lead to improved understanding of the role of land surface processes in the unique climatic and environmental conditions in this complex region, and would be an essential first step to applications such as climate impacts of land-use changes or land-data assimilation. Additionally, comparative studies could evaluate Noah-MP's performance against other land surface models, such as the Joint UK Land Environment Simulator (JULES) and the Community Terrestrial System Model (CTSM). These comparisons would provide valuable insights into how different land surface schemes influence model performance in tropical regions.

4.1.2 Inclusion of missing vegetation and soil processes into Noah-MP

Noah-MP's inability to simulate the coexistence of multiple tropical forest species may contribute to discrepancies between calibrated LH and SH. Tropical forests are characterized by high biodiversity, including species with varying ages, sizes, and functional traits. These factors are essential for accurately representing energy, water, and carbon cycling as well as ecosystem functions (Cheng et al., 2024b). Incorporating more advanced ecosystem demography models into Noah-MP would allow for better simulation of these ecosystem dynamics. Additionally, the absence of an organic soil layer can contribute to the model's overestimation of nighttime soil temperatures, highlighting another important area for future development.

4.1.3 Inclusion of missing hydrological processes into Noah-MP

The absence of preferential flow pathways, which are formed by tree roots and earthworm burrows, is another likely source of structural error in Noah-MP. These pathways are prevalent in tropical regions and play a crucial role in rainfall partitioning and hydrological responses (Cheng et al., 2017; 2018). Their exclusion may undermine model calibration efforts for surface heat fluxes. Despite their importance, these processes remain underrepresented in land surface models and should be prioritized in future model improvement efforts.

A notable limitation of Noah-MP-SLUCM is its lack of urban hydrology, which leads to significant biases in simulating hydrological processes over urban areas. Future research should address this gap by developing and integrating urban hydrology modules, particularly for tropical urban regions.

4.2 Broader implications for model development and benchmarking

This study illustrates a transferable approach for identifying parameter sensitivities and calibration priorities in data-scarce tropical environments. While the analysis was conducted at three distinct sites, the framework for parameter selection, calibration, and evaluation can be extended to other tropical regions with similar climatic or ecological characteristics. The findings underscore the need for modular model structures that allow targeted refinement without full structural overhaul. In doing so, this work supports ongoing efforts to benchmark and systematically improve land surface model components, particularly in regions where empirical constraints are sparse but climate sensitivity is high.



5 Conclusions

This study demonstrates that site-specific calibration using local observations significantly improves Noah-MP's ability to simulate land surface processes in tropical environments, relative to its default parameterization. Across tropical forest and urban sites, observation-driven calibrated simulations yield better representations of latent and sensible heat fluxes and soil moisture at both daily and seasonal timescales. Sensitivity analyses highlight a consistent set of key vegetation and soil parameters in tropical forests, including VCMX25, LAI, SATDK, and REFSMC, that often dominate model performance and could be prioritized for tuning in similar settings.

Despite improvements, persistent model biases reveal structural limitations that cannot always be resolved through calibration alone. In tropical forests, Noah-MP fails to adequately capture dry-season soil moisture decline, wet-season soil moisture peaks, and latent heat variability likely due to the deficiencies in subsurface water transport representation and the lack of multi-species vegetation representation. Persistent overestimation of nighttime sensible heat further underscores structural deficiencies, such as the omission of organic soil layers that buffer diurnal temperature variations. Similarly, in tropical urban settings, substantial latent heat biases stem from simplified hydrological assumptions in the Noah-MP-SLUCM scheme, including no infiltration and no treatment of irrigated or pervious surfaces in urban areas. Furthermore, efforts to improve one energy flux often degrade another, reflecting energy partitioning trade-offs and internal coupling limitations, particularly under strong seasonal forcing, as seen in Panama. Moreover, calibrated parameter sets are likely not directly transferable across sites, even within the same biome, due to differences in canopy structure, land cover composition, and seasonal behavior of water and energy fluxes.

These findings underscore the importance of regionally adaptive calibration strategies informed by local data, while also pointing to the need for structural model development in hydrology, vegetation, and urban land surface representation to ensure reliable land-atmosphere simulations in data-scarce, climate-sensitive tropical regions.

Acknowledgments: We thank Hailin Yan (now at Bureau of Meteorology, Australia) and Jerry Liu (Centre for Climate Research Singapore) for technical support. The collection of the PSO data used in this study was supported by the JSPS KAKENHI (Grant number 24K01813).

Code and data availability statement: The current version of Noah-MP model is available from <https://github.com/NCAR/hrldas>. The exact version of the model used to produce the results used in this paper is archived on repository under 10.5281/zenodo.16780672 (Cheng 2025a). The flux tower data at the Malaysia PSO site is available at: https://asiaflux.net/index.php?page_id=93. The flux tower data at the Singapore site is available at: <https://doi.org/10.5281/zenodo.7104984> (Lipson et al., 2022). The data produced by the simulations in this study is available from <https://zenodo.org/records/16022303> (Cheng 2025b).



430 *Author contribution:* YC, KF, CH, FC, and AZ contributed to conceptualization, methodology, and investigation. YC led the simulation, investigation, data curation, and visualization. MD, YM, BP, YK, ML, SN, ST, LM, and BZ provided resources. YC led the writing of this manuscript with contributions from all authors. All authors read and approved the final manuscript.

References

- 435 Arsenault, K. R., Nearing, G. S., Wang, S., Yatheendradas, S., and Peters-Lidard, C. D. (2018). Parameter sensitivity of the Noah-MP land surface model with dynamic vegetation. *Journal of Hydrometeorology*, 19(5), 815–830. <https://doi.org/10.1175/JHM-D-17-0205.1>
- Bonan. (1995). Land-Atmosphere interactions for climate system Models: coupling biophysical, biogeochemical, and ecosystem dynamical processes. *Remote Sensing of Environment*, 51(1), 57–73. [https://doi.org/10.1016/0034-4257\(94\)00065-U](https://doi.org/10.1016/0034-4257(94)00065-U)
- 440 Bonan, and Doney, S. (2018). Climate, ecosystems, and planetary futures: The challenge to predict life in Earth system models. *Science*, 359(6375). <https://doi.org/10.1126/science.aam8328>
- Chang, M., Liao, W., Wang, X., Zhang, Q., Chen, W., Wu, Z., and Hu, Z. (2020). An optimal ensemble of the Noah-MP land surface model for simulating surface heat fluxes over a typical subtropical forest in South China. *Agricultural and Forest Meteorology*, 281(November 2019), 107815. <https://doi.org/10.1016/j.agrformet.2019.107815>
- 445 Chen, D. X., Ban, X. Q., Li, Y. De, Xiao, W. F., Luo, T. S., Lin, M. X., and Xu, H. (2008). Responses of gas exchange to neighborhood interference in leaves of teak (*Tectona grandis* L. f.) in a tropical plantation forest. *Shengtai Xuebao/ Acta Ecologica Sinica*, 28(9), 4059–4069. [https://doi.org/10.1016/s1872-2032\(08\)60078-5](https://doi.org/10.1016/s1872-2032(08)60078-5)
- Chen, F., Bornstein, R., and Al, E. (2011). The Integrated WRF / Urban Modeling System : Development , Evaluation , and Applications to Urban Environmental Problems. *International Journal of Climatology*, 31(2), 273–288.
- 450 Cheng, Ogden, F., and Zhu, J. (2017). Earthworms and tree roots: A model study of the effect of preferential flow paths on runoff generation and groundwater recharge in steep, saprolitic, tropical lowland catchments. *Water Resources Research*, 53(7), 5400–5419. <https://doi.org/10.1002/2016WR020258>
- Cheng, Y, Huang, M., Chen, M., Guan, K., Bernacchi, C., Peng, B., and Tan, Z. (2020). Parameterizing Perennial Bioenergy Crops in Version 5 of the Community Land Model Based on Site-Level Observations in the Central Midwestern United States. *Journal of Advances in Modeling Earth Systems*, 12(1), 1–24. <https://doi.org/10.1029/2019MS001719>
- 455 Cheng, Y, Leung, L. R., Huang, M., Koven, C., Detto, M., Knox, R., et al. (2022). Modeling the joint effects of vegetation characteristics and soil properties on ecosystem dynamics in a Panama tropical forest. *Journal of Advances in Modeling Earth Systems*. <https://doi.org/10.1029/2021ms002603>
- 460 Cheng, Yanyan, Ogden, F. L., Zhu, J., and Bretfeld, M. (2018). Land use dependent preferential flow paths affect hydrological response of steep tropical lowland catchments with saprolitic soils. *Water Resources Research*.



<https://doi.org/10.1029/2017WR021875>

Cheng, Yanyan, Ogden, F., and Zhu, J. (2019). Characterization of sudden and sustained base flow jump hydrologic behaviour in the humid seasonal tropics of the Panama Canal Watershed. *Hydrological Processes*, (April), 1–14.

<https://doi.org/10.1002/hyp.13604>

Cheng, Yanyan, Huang, M., Lawrence, D. M., Calvin, K., Lombardozzi, D. L., Sinha, E., et al. (2022). Future bioenergy expansion could alter carbon sequestration potential and exacerbate water stress in the United States. *Science Advances*, 8(18), 1–14. <https://doi.org/DOI: 10.1126/sciadv.abm8237>

Cheng, Yanyan, Xia, W., Detto, M., and Shoemaker, C. A. (2023). A framework to calibrate ecosystem demography models within Earth system models using parallel surrogate global optimization. *Water Resources Research*. <https://doi.org/10.1029/2022WR032945>

Cheng, Yanyan, Lawrence, D. M., Pan, M., Zhang, B., Graham, N. T., Lawrence, P. J., et al. (2024a). A bioenergy-focused versus a reforestation-focused mitigation pathway yields disparate carbon storage and climate responses. *Proceedings of the National Academy of Sciences*, 121(7), 1–11. <https://doi.org/10.1073/pnas.2306775121>

Cheng, Yanyan, Wang, W., Detto, M., Fisher, R., and Shoemaker, C. (2024b). Calibrating Tropical Forest Coexistence in Ecosystem Demography Models Using Multi-Objective Optimization Through Population-Based Parallel Surrogate Search. *Journal of Advances in Modeling Earth Systems*, 16(8), 1–18. <https://doi.org/10.1029/2023MS004195>

Cheng, Yanyan, (2025a). Noah-MP.Cheng. Zenodo. <https://zenodo.org/records/16780672>

Cheng, Yanyan, (2025b). Simulation results for "Assessing and enhancing Noah-MP land surface modeling over tropical environments". Zenodo. <https://zenodo.org/records/16022303>

Cheruy, F., Dufresne, J. L., Hourdin, F., and Ducharne, A. (2014). Role of clouds and land-atmosphere coupling in midlatitude continental summer warm biases and climate change amplification in CMIP5 simulations. *Geophysical Research Letters*, 41(18), 6493–6500. <https://doi.org/10.1002/2014GL061145>

Cox, P. M., Betts, R. A., Bunton, C. B., Essery, R. L. H., Rowntree, P. R., and Smith, J. (1999). The impact of new land surface physics on the GCM simulation of climate and climate sensitivity. *Climate Dynamics*, 15(3), 183–203. <https://doi.org/10.1007/s003820050276>

Cox, P. M., Betts, R. A., Jones, C. D., and Spall, S. A. (2000). Acceleration of global warming due to carbon-cycle feedbacks in a coupled climate model. *Nature*, 408(November), 184–187.

Crossley, J. F., Polcher, J., Cox, P. M., Gedney, N., and Planton, S. (2000). Uncertainties linked to land-surface processes in climate change simulations. *Climate Dynamics*, 16(12), 949–961. <https://doi.org/10.1007/s003820000092>

Detto, M., and Pacala, S. W. (2022). Plant hydraulics, stomatal control, and the response of a tropical forest to water stress over multiple temporal scales. *Global Change Biology*, 28(14), 4359–4376. <https://doi.org/10.1111/gcb.16179>

Detto, M., Asner, G. P., Muller-Landau, H. C., and Oliver Sonnentag. (2015). Spatial variability in tropical forest leaf area density from multireturn lidar and modeling. *Journal of Geophysical Research: Biogeosciences*, 120, 965–978. <https://doi.org/10.1002/2014JG002774>.Received



- Dickinson, R. E. (1983). Land surface processes and climate—surface albedos and energy balance. *Advances in Geophysics*, 25(C), 305–353. [https://doi.org/10.1016/S0065-2687\(08\)60176-4](https://doi.org/10.1016/S0065-2687(08)60176-4)
- Domingues, T. F., Berry, J. A., Martinelli, L. A., Ometto, J. P. H. B., and Ehleringer, J. R. (2005). Parameterization of canopy structure and leaf-level gas exchange for an Eastern Amazonian tropical rain forest (Tapajós national forest, Pará, Brazil). *Earth Interactions*, 9(17). <https://doi.org/10.1175/EI149.1>
- 500 Fang, Y., Leung, L. R., Koven, C. D., Bisht, G., Detto, M., Cheng, Y., et al. (2022). Modeling the topographic influence on aboveground biomass using a coupled model of hillslope hydrology and ecosystem dynamics. *Geoscientific Model Development*, 15(20), 7879–7901. <https://doi.org/10.5194/gmd-15-7879-2022>
- Fisher, R., and Koven, C. (2020). Perspectives on the Future of Land Surface Models and the Challenges of Representing Complex Terrestrial Systems. *Journal of Advances in Modeling Earth Systems*, 12(4). <https://doi.org/10.1029/2018ms001453>
- 505 Gao, M., Chen, F., Shen, H., Barlage, M., Li, H., Tan, Z., and Zhang, L. (2019). Efficacy of possible strategies to mitigate the urban heat island based on urbanized high-resolution land data assimilation system (U-HRLDAS). *Journal of the Meteorological Society of Japan*, 97(6), 1075–1097. <https://doi.org/10.2151/jmsj.2019-060>
- 510 Gentine, P., Massmann, A., Lintner, B. R., Alemohammad, S. H., Fu, R., Green, J. K., et al. (2019). Land–atmosphere interactions in the tropics – a review, 4171–4197.
- Goudriaan, J. (1977). Crop micrometeorology: a simulation study. *Wageningen University and Research*.
- Hasler, N., Williams, C. A., Denney, V. C., Ellis, P. W., Shrestha, S., Hart, D. E. T., et al. (2024). Accounting for albedo change to identify climate-positive tree cover restoration. *Nature Communications*, (December 2023), 1–11. <https://doi.org/10.1038/s41467-024-46577-1>
- 515 He, C., Valayamkunnath, P., Barlage, M., Chen, F., Gochis, D., Cabell, R., et al. (2023a). Modernizing the open-source community Noah with multi-parameterization options (Noah-MP) land surface model (version 5.0) with enhanced modularity, interoperability, and applicability. *Geoscientific Model Development*, 16(17), 5131–5151. <https://doi.org/10.5194/gmd-16-5131-2023>
- 520 He, C., Chen, F., Barlage, M., Yang, Z. L., Wegiel, J. W., Niu, G. Y., et al. (2023b). Enhancing the Community Noah-MP Land Model Capabilities for Earth Sciences and Applications. *Bulletin of the American Meteorological Society*, 104(11), E2023–E2029. <https://doi.org/10.1175/BAMS-D-23-0249.1>
- He, C., Valayamkunnath, P., Barlage, M., Chen, F., Yang, Z., Niyogi, D., and Michael, E. (2023c). The Community Noah-MP Land Surface Modeling System Technical Description Version 5.0, 284. <https://doi.org/https://doi.org/10.5065/ew8g-yr95>
- 525 Huang, M., Ray, J., Hou, Z., Ren, H., Liu, Y., and Swiler, L. (2016). On the applicability of surrogate-based Markov chain Monte Carlo-Bayesian inversion to the Community Land Model: Case studies at flux tower sites. *Journal of Geophysical Research: Atmospheres*, 121, 7548–7563. <https://doi.org/https://doi.org/10.1002/2015JD024339>
- Kennedy, D., Dagon, K., Lawrence, D. M., Fisher, R. A., Benjamin, M., Collier, N., et al. (2024). One-at-a-time Parameter



- 530 Perturbation Ensemble of the Community Land Model , version 5.1.
- Kosugi, Y., Takanashi, S., Yokoyama, N., Philip, E., and Kamakura, M. (2012). Vertical variation in leaf gas exchange parameters for a Southeast Asian tropical rainforest in Peninsular Malaysia. *Journal of Plant Research*, 125(6), 735–748. <https://doi.org/10.1007/s10265-012-0495-5>
- Lambin, E. F., Geist, H. J., and Lepers, E. (2003). Dynamics of Land-Use and Land-Cover Change in Tropical Regions. *Annual*
535 *Review of Environment and Resources*, 28(1), 205–241. <https://doi.org/10.1146/annurev.energy.28.050302.105459>
- Lawrence, P., Feddema, J., Bonan, G., Meehl, G., O'Neill, B., Oleson, K., et al. (2012). Simulating the biogeochemical and biogeophysical impacts of transient land cover change and wood harvest in the Community Climate System Model (CCSM4) from 1850 to 2100. *Journal of Climate*, 25(9), 3071–3095. <https://doi.org/10.1175/JCLI-D-11-00256.1>
- Li, X., Koh, T., Panda, J., and Norford, L. K. (2016). Impact of urbanization patterns on the local climate of a tropical city ,
540 Singapore: An ensemble study. *Journal of Geophysical Research: Atmospheres*, 121(9), 4386–4403. <https://doi.org/10.1002/2015JD024452>.Received
- Lin, Y., Dong, W., Zhang, M., Xie, Y., Xue, W., Huang, J., and Luo, Y. (2017). Causes of model dry and warm bias over central U.S. and impact on climate projections. *Nature Communications*, 8(1), 1–8. <https://doi.org/10.1038/s41467-017-01040-2>
- 545 Lion, M., Kosugi, Y., Takanashi, S., Noguchi, S., Itoh, M., Katsuyama, M., et al. (2017). Evapotranspiration and water source of a tropical rainforest in peninsular Malaysia. *Hydrological Processes*, 31(24), 4338–4353. <https://doi.org/10.1002/hyp.11360>
- Lipson, M., Grimmond, S., Best, M., Chow, W. T. L., Christen, A., Chrysoulakis, N., et al. (2022). Harmonized gap-filled datasets from 20 urban flux tower sites. *Earth System Science Data*, 14(11), 5157–5178. [https://doi.org/10.5194/essd-](https://doi.org/10.5194/essd-14-5157-2022)
550 [14-5157-2022](https://doi.org/10.5194/essd-14-5157-2022)
- Litt, G. F., Ogden, F. L., Mojica, A., Hendrickx, J. M. H., Kempema, E. W., Gardner, C. B., et al. (2020). Land cover effects on soil infiltration capacity measured using plot scale rainfall simulation in steep tropical lowlands of Central Panama. *Hydrological Processes*, 34(4), 878–897. <https://doi.org/10.1002/hyp.13605>
- Lu, D., and Ricciuto, D. (2019). Efficient surrogate modeling methods for large-scale Earth system models based on machine
555 learning techniques. *Geoscientific Model Development*, 1791–1807. [https://doi.org/https://doi.org/10.5194/gmd-12-1791-2019](https://doi.org/10.5194/gmd-12-1791-2019)
- Lu, D., Ricciuto, D., Stoyanov, M., and Gu, L. (2018). Calibration of the E3SM Land Model Using Surrogate-Based Global Optimization. *Journal of Advances in Modeling Earth Systems*, 10(6), 1337–1356. <https://doi.org/10.1002/2017MS001134>
- 560 Lu, D., Liu, Y., Zhang, Z., Bao, F., and Zhang, G. (2024). A Diffusion-Based Uncertainty Quantification Method to Advance E3SM Land Model Calibration. *Journal of Geophysical Research: Machine Learning and Computation*, 1(3). <https://doi.org/10.1029/2024jh000234>
- Ma, H. Y., Mechoso, C. R., Xue, Y., Xiao, H., Neelin, J. D., and Ji, X. (2013). On the connection between continental-scale



- land surface processes and the tropical climate in a coupled ocean-atmosphere-land system. *Journal of Climate*, 26(22), 9006–9025. <https://doi.org/10.1175/JCLI-D-12-00819.1>
- 565 Mahmood, R., Pielke, R. A., Hubbard, K. G., Niyogi, D., Dirmeyer, P. A., McAlpine, C., et al. (2014). Land cover changes and their biogeophysical effects on climate. *International Journal of Climatology*, 34(4), 929–953. <https://doi.org/10.1002/joc.3736>
- 570 Marryanna, L., S. Noguchi, Y. Kosugi, K. Niiyama, M. Itoh, T. Sato, S. Takanashi, S. Siti-Aisah, and K. A.-R. (2019). Spatial Distribution of Soil Moisture and Its Influence on Stand Structure in a Lowland Dipterocarp Forest in Peninsular Malaysia. *Journal of Tropical Forest Science*, 31(2), 135–150.
- Müller, J., Paudel, R., Shoemaker, C. A., Woodbury, J., Wang, Y., and Mahowald, N. (2015). CH₄ parameter estimation in CLM4.5bgc using surrogate global optimization. *Geoscientific Model Development*, 8(10), 3285–3310. <https://doi.org/10.5194/gmd-8-3285-2015>
- 575 Newman, A. J., Kalb, C., Chakraborty, T. C., Fitch, A., Darrow, L. A., Warren, J. L., et al. (2024). The High-resolution Urban Meteorology for Impacts Dataset (HUMID) daily for the Conterminous United States. *Scientific Data*, 11(1), 1–16. <https://doi.org/10.1038/s41597-024-04086-2>
- Niu, G. Y., Yang, Z. L., Mitchell, K. E., Chen, F., Ek, M. B., Barlage, M., et al. (2011). The community Noah land surface model with multiparameterization options (Noah-MP): 1. Model description and evaluation with local-scale measurements. *Journal of Geophysical Research Atmospheres*, 116(12), 1–19. <https://doi.org/10.1029/2010JD015139>
- 580 Noguchi, S., Kosugi, Y., Takanashi, S., Tani, M., Niiyama, K., Siti Aisah, S., and Lion, M. (2016). Long-term variation in soil moisture in Pasoh forest reserve, a lowland tropical rainforest in Malaysia. *Journal of Tropical Forest Science*, 28(5), 324–333.
- Ogden, F. L., Crouch, T. D., Stallard, R. F., and Hall, J. S. (2013). Effect of land cover and use on dry season river runoff, runoff efficiency, and peak storm runoff in the seasonal tropics of Central Panama. *Water Resources Research*, 49(12), 8443–8462. <https://doi.org/10.1002/2013WR013956>
- 585 Pan, Y., Birdsey, R. A., Fang, J., Houghton, R., Kauppi, P. E., Kurz, W. A., and Phillip, O. L. (2011). A Large and Persistent Carbon Sink in the World's Forests. *Science*, 333(6045), 988–993. Retrieved from 10.1126/science.1201609
- Pielke, R. A., Pitman, A., Niyogi, D., Mahmood, R., McAlpine, C., Hossain, F., et al. (2011). Land use/land cover changes and climate: Modeling analysis and observational evidence. *Wiley Interdisciplinary Reviews: Climate Change*, 2(6), 828–850. <https://doi.org/10.1002/wcc.144>
- 590 Pitman, A. J., De Noblet-Ducoudré, N., Cruz, F. T., Davin, E. L., Bonan, G. B., Brovkin, V., et al. (2009). Uncertainties in climate responses to past land cover change: First results from the LUCID intercomparison study. *Geophysical Research Letters*, 36(14), 1–6. <https://doi.org/10.1029/2009GL039076>
- 595 Roth, M., Jansson, C., and Velasco, E. (2017). Multi-year energy balance and carbon dioxide fluxes over a residential neighbourhood in a tropical city. *International Journal of Climatology*, 37(5), 2679–2698. <https://doi.org/10.1002/joc.4873>



- Salamanca, F., Zhang, Y., Barlage, M., Chen, F., Mahalov, A., and Miao, S. (2018). Evaluation of the WRF-Urban Modeling System Coupled to Noah and Noah-MP Land Surface Models Over a Semiarid Urban Environment. *Journal of Geophysical Research: Atmospheres*, 123(5), 2387–2408. <https://doi.org/10.1002/2018JD028377>
- Schlesinger, W. H., and Jasechko, S. (2014). Transpiration in the global water cycle. *Agricultural and Forest Meteorology*, 189–190, 115–117. <https://doi.org/10.1016/j.agrformet.2014.01.011>
- Shao, R., and Zhang, B. (2019). Estimating the Increase in Regional Evaporative Water Consumption as a Result of Vegetation Restoration Over the Loess Plateau, China. *Journal of Geophysical Research: Atmospheres*, 783–802. <https://doi.org/10.1029/2019JD031295>
- Sun, R., Duan, Q., and Huo, X. (2021). Multi-Objective Adaptive Surrogate Modeling-Based Optimization for Distributed Environmental Models Based on Grid Sampling. *Water Resources Research*, 57(11). <https://doi.org/10.1029/2020WR028740>
- Sun, W., Wang, B., and Wang, Y. (2021). Parameterizing Subgrid Variations of Land Surface Heat Fluxes to the Atmosphere Improves Boreal Summer Land Precipitation Simulation With the NCAR CESM1.2. *Geophysical Research Letters*. *Geophysical Research Letters*, 48, 1–10. <https://doi.org/10.1029/2020GL090715>
- Unger, N. (2014). Human land-use-driven reduction of forest volatiles cools global climate. *Nature Climate Change*, 4(10), 907–910. <https://doi.org/10.1038/nclimate2347>
- Vetrita, Y., and Cochrane, M. A. (2020). Fire frequency and related land-use and land-cover changes in Indonesia's Peatlands. *Remote Sensing*, 12(1). <https://doi.org/10.3390/RS12010005>
- Van Weverberg, K., Morcrette, C. J., Petch, J., Klein, S. A., Ma, H. Y., Zhang, C., et al. (2018). CAUSES: Attribution of Surface Radiation Biases in NWP and Climate Models near the U.S. Southern Great Plains. *Journal of Geophysical Research: Atmospheres*, 123(7), 3612–3644. <https://doi.org/10.1002/2017JD027188>
- Xue, L., Kusaka, H., He, C., and Chen, F. (2024). Insights Into Urban Heat Island and Heat Waves Synergies Revealed by a Land-Surface-Physics-Based Downscaling Method. <https://doi.org/10.1029/2023JD040531>
- Yang, Z. L., Niu, G. Y., Mitchell, K. E., Chen, F., Ek, M. B., Barlage, M., et al. (2011). The community Noah land surface model with multiparameterization options (Noah-MP): 2. Evaluation over global river basins, 116, 1–16. <https://doi.org/10.1029/2010JD015140>
- Zhang, B., Tian, L., Yang, Y., and He, X. (2022). Revegetation Does Not Decrease Water Yield in the Loess Plateau of China. *Geophysical Research Letters*, 49(9). <https://doi.org/10.1029/2022GL098025>
- Zhang, G., Chen, Y., and Li, J. (2021). Effects of organic soil in the Noah-MP land-surface model on simulated skin and soil temperature profiles and surface energy exchanges for China. *Atmospheric Research*, 249(September 2020). <https://doi.org/10.1016/j.atmosres.2020.105284>